Annals of Nuclear Medicine Vol. 20, No. 8, 511–517, 2006

Effect of linearization correction on statistical parametric mapping (SPM): A ^{99m}Tc-HMPAO brain perfusion SPECT study in mild Alzheimer's disease

Md. Ashik B. Ansar,*,** Yasuhiro Osaki,* Hiroaki Kazui,** Naohiko Oku,* Masashi Takasawa,* Yasuyuki Kimura,* Nurun N. Begum,** Yoshitaka Ikejiri,** Masatoshi Takeda** and Jun Hatazawa*

*Department of Nuclear Medicine and Tracer Kinetics, Osaka University Graduate School of Medicine
**Department of Psychiatry and Behavioral Proteomics, Osaka University Graduate School of Medicine

Objective: Statistical parametric mapping (SPM) was employed to investigate the regional decline in cerebral blood flow (rCBF) as measured by ^{99m}Tc-hexamethyl propylene amine oxime (HMPAO) single photon emission computed tomography (SPECT) in mild Alzheimer's disease (AD). However, the role of the post reconstruction image processing on the interpretation of SPM, which detects rCBF pattern, has not been precisely studied. We performed ^{99m}Tc-HMPAO SPECT in mild AD patients and analyzed the effect of linearization correction for washout of the tracer on the detectability of abnormal perfusion. ***Methods:*** Eleven mild AD (NINCDS-ADRDA, male/female, 5/6; mean ± SD age, 70.6 ± 6.2 years; mean ± SD mini-mental state examination score, 23.9 ± 3.41; clinical dementia rating score, 1) and eleven normal control subjects (male/female, 4/7; mean ± SD age, 66.8 ± 8.4 years) were enrolled in this study. ^{99m}Tc-HMPAO SPECT was performed with a four-head rotating gamma camera. We employed linearization uncorrected (LU) and linearization corrected (LC) images for the patients and controls. The pattern of hypoperfusion in mild AD on LU and LC images was detected by SPM99 applying the same image standardization and analytical parameters. A statistical inter image-group analysis (LU vs. LC) was also performed. ***Results:*** Clear differences were observed between the interpretation of SPM with LU and LC images. Significant hypoperfusion in mild AD was found on the LU images in the left posterior cingulate gyrus, right precuneus, left hippocampus, left uncus, and left superior temporal gyrus (cluster level, corrected $p < 0.005$). With the LC images, significant hypoperfusion in AD was found only in the bilateral posterior cingulate gyrus and left precuneus (cluster level, corrected $p < 0.005$). A pattern of greater rCBF distribution at the high flow cortices and low flow cortices was observed on LC and LU images, respectively, in the case of both controls and mild AD patients. ***Conclusion:*** Hippocampal hypoperfusion could be detected by means of SPM in the LU images but not in the LC images. The results of SPM may vary in ^{99m}Tc-HMPAO SPECT with or without linearization correction, which should be carefully evaluated when interpreting the pattern of rCBF changes in mild Alzheimer's disease.

Key words: Alzheimer's disease, linearization-correction, ^{99m}Tc-HMPAO SPECT, regional cerebral blood flow, statistical parametric mapping

INTRODUCTION

Brain perfusion imaging by means of ^{99m}Tc-labeled hexamethyl propylene amine oxime (HMPAO) single photon emission computed tomography (SPECT) has been employed for the diagnosis of Alzheimer's disease and has a useful predictive value over the clinical diagnostic criteria in AD.[1,2] However, visual inspection alone is unable to quantify changes of image intensity to differentiate any small change in the regional cerebral blood flow (rCBF).[3] Although quantitative analysis like region of interest (ROI) has gained some general acceptance, it has some limitations with its a priori anatomical hypothesis

Received February 24, 2006, revision accepted June 22, 2006.
For reprint contact: Jun Hatazawa, M.D., Ph.D., Department of Nuclear Medicine and Tracer Kinetics, Osaka University Graduate School of Medicine, 2–2 Yamadaoka, Suita, Osaka 565–0871, JAPAN.
E-mail: hatazawa@tracer.med.osaka-u.ac.jp

leaving large areas of unexplored brain structures.[4] The combination of SPECT and statistical parametric mapping (SPM)[5] can analyze spatially normalized images by plotting them against standard stereotactic space thereby allowing a voxel by voxel statistical test to delineate more objective and reliable assessment of the pattern of the rCBF changes that occur in AD. Moreover, SPM decreases the limitation in inter-rater variability and increases the accuracy of diagnosis, which may be considered effective in routine clinical settings.[6]

^{99m}Tc-HMPAO-associated brain distribution behavior is known to be non-linearly correlated to the rCBF due to a certain magnitude of flow dependent back diffusion of lipophilic ^{99m}Tc-HMPAO from the brain to the blood that can occur prior to measurement with SPECT. This causes a saturation effect, as a result of which the radioactivity count does not increase proportionally with the increase in the rCBF. Linearization-correction is an image processing method that applies Lassen's algorithm[7] on each SPECT voxel to enhance the image contrast in a post-processing manner. Thus, the method corrects the saturation effect to obtain a more direct proportionality between the corrected-count (image intensity) and blood flow without influencing spatial resolution on tomographic images.[7] Therefore, this technique has been widely accepted for cerebral perfusion studies in stroke and related diseases. To detect the pattern of rCBF changes in mild AD, the linearization correction method was adopted by some study groups[8,9] however, not by others.[10–14] Since it has been already reported that image reconstruction methods might influence the sensitivity of SPM,[15] in that concern it would be important to know whether linearization-correction affects SPM analysis or, that to be used for detecting the earliest perfusion changes occurring in mild AD. The current study addressed this issue. Moreover, to date, no one has paid attention to the detectability of the pattern of abnormal brain perfusion on ^{99m}Tc-HMPAO SPECT with or without linearization correction. Hence, the aim of the present study was to evaluate the interpretations of SPM analyses on the ^{99m}Tc-HMPAO SPECT with or without linearization correction while detecting the pattern of rCBF changes in mild AD.

MATERIALS AND METHODS

Subjects

Eleven patients were enrolled in the study (male/female, 5/6; mean ± SD age, 70.6 ± 6.2 years) all of whom had visited the psychiatric outpatient department in Osaka University Medical Hospital, Osaka, Japan, with memory complaints. All patients met the National Institute of Neurological and Communicative Disorders and Stroke Alzheimer's Disease and Related Disorders Association (NINCDS-ADRDA) criteria for probable AD.[16] Patient's Mini-Mental State Examination (MMSE) score was mean ± SD, 23.9 ± 3.4 and severity of dementia based on the Clinical Dementia Rating (CDR) was determined as 1 (mild).[17] Eleven normal controls (NC) (male/female, 4/7; mean ± SD age, 66.8 ± 8.4 years) underwent a thorough screening. All subjects were thoroughly examined with general and neurological examinations together with cranial magnetic resonance imaging (MRI) to exclude any complications related to other neurological, cardiovascular, and renal impairments and to elucidate evidence of developmental abnormalities or significant neurological antecedents. This project was approved by the Review Committee of Osaka University Hospital, Osaka, Japan. The study was performed in compliance with the Declaration of Helsinki.

SPECT imaging

The SPECT studies were performed using four-head rotating gamma cameras (GAMMA VIEW SPECT 2000H; Hitachi Medical Corporation, Tokyo, Japan). In-plane and axial resolution of the camera was 10.0 mm full width at half maximum (FWHM). The scanner was equipped with a low energy high resolution parallel-hole collimator.[18] SPECT was initiated within 10 minutes after injection of approximately 740 MBq (20 mCi) ^{99m}Tc-HMPAO and the acquisition was done at 8 s per step, with 128 collections over 360°. The final data set consisted of 64 × 64 matrix (4 × 4 mm per pixel, 4 mm thickness) from the sum total of data acquired by the four cameras.[19] Each subject was placed in the supine position on the scanning bed with eyes closed during injection and subsequent scanning period in a quiet, dimly lit examination room. A synthetic headband fixed to the headrest was applied to minimize head movement during scanning. The raw SPECT data were transferred to a nuclear medicine computer (HARP-3, Hitachi Medical Corporation, Tokyo, Japan). Projection data were pre-filtered with a Butterworth low pass filter (Order 10, cutoff frequency 0.20 cycles/pixel) to minimize noise, and then reconstructed into transaxial sections of 4.0 mm thick slice in-plane parallel to the orbitomeatal line using a Filtered Back Projection algorithm. Chang's first order post-processing attenuation correction[20] was applied to images reconstructed using 0.08 cm^{-1} as a routine attenuation coefficient in the clinical setting.[21] Thus, linearization-uncorrected (LU) images were reconstructed (64 × 64 matrix, 4 mm slice thickness, transaxial oblique in-plane parallel to orbitomeatal line). On the other hand, for linearization-correction, after completing the identical procedures up to the attenuation correction, we applied Lassen's algorithm. Lassen's algorithm is represented by the equation $Fi/Fr = \alpha(Ci/Cr)/[1 + \alpha - (Ci/Cr)]$, where Fi/Fr is a ratio of CBF in each region to that in a reference region and Ci/Cr is the ratio of count activity in each region to that in a reference region.[7] Alpha (α) is the ratio between the rate of the back diffusion of the diffusible lipophilic ^{99m}Tc-HMPAO from the brain to the blood and the rate of conversion of the lipophilic compound to the hydrophilic

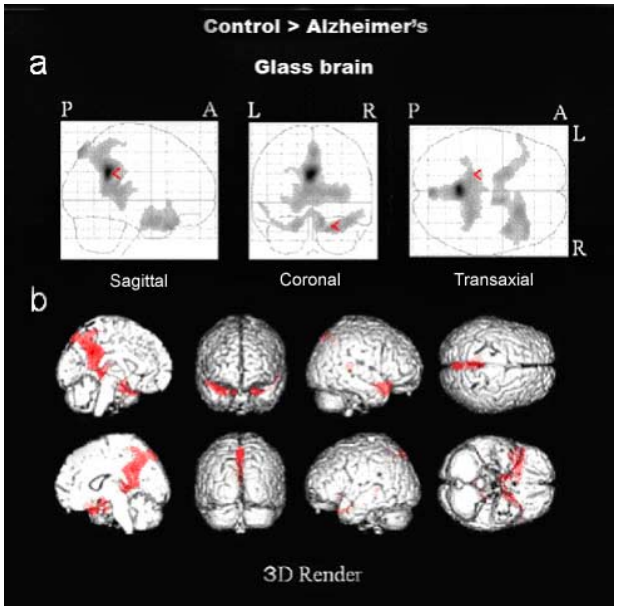

Fig. 1

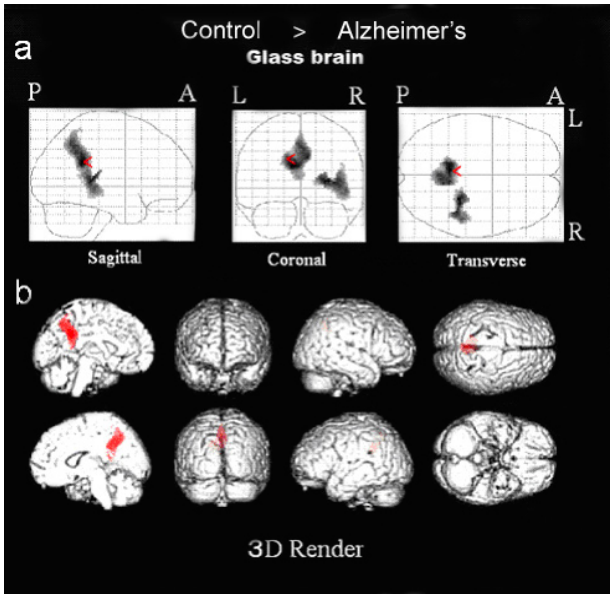

Fig. 2

Fig. 1 and Fig. 2 SPM99 corrected for multiple comparisons ($p < 0.05$). Images show lower regional cerebral blood flow (rCBF) in the mild AD in comparison with that in the healthy volunteer when LU (Fig. 1) and LC (Fig. 2) images are used for the analysis. The difference in the rCBF distribution is shown as (a) in the three orthogonal projections in the glass brain and (b) the colored areas superimposed on volume rendering of standard 3-dimension anatomic template of magnetic resonance images (3D Render). P, A, L and R represent posterior, anterior, left and right respectively.

form. We used 1.5 as the value for α which was validated in other studies.[22,23] The cerebellum was defined as a reference region according to Yonekura et al.[23] consider-

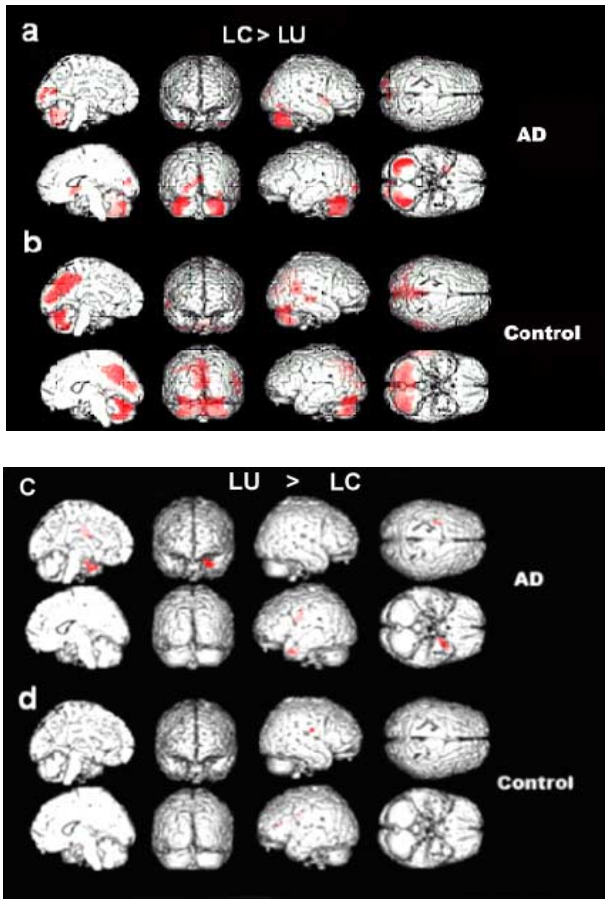

Fig. 3 SPM demonstrates the difference in rCBF distribution between the LU and LC images as indicated by the colored areas superimposed on volume rendering of standard 3-dimension anatomic template of magnetic resonance images (3D Render). The contrast, LC > LU, reflects that (a, b) the pattern of rCBF distribution is less in LU images or high in LC images, whereas, the contrast, LU > LC, reflects that (c, d) the pattern of rCBF distribution is less in LC images or high in LU images.

ing that cerebellar blood flow is not impaired severely in AD.[24,25] Final image resolution of LC images was 64 × 64 matrix, 4 mm slice thickness, transaxial oblique in-plane parallel to orbitomeatal line.

Data analysis

The transverse slice volumes of both the LU and LC ^{99m}Tc-HMPAO SPECT images were transformed into the 'ANALYZE format' before going to SPM (Wellcome Department of Cognitive Neurology, London, UK) on MATLAB (Math Works, Inc., Natic, MA, USA). All images (LU and LC) were transformed to the standard anatomic space[26] with the SPECT template image of SPM99 and smoothed by three-dimensional convolution with an isotropic Gaussian Kernel (FWHM: 12 mm). The statistical model "Compare population: 1 scan/subject" was chosen to perform voxel by voxel two sample t-tests

Table 1 Locations and peaks observed in SPM showing hypoperfusion in Alzheimer's disease

SPM	Image group	Set level p	Cluster level		Peak voxels					
			K_E	Corrected p	Locations	BA	x	y	z	Z-score
NC > AD	LU	0.021	3863	0.000	Left posterior cingulate	29	−2	45	28	5.49
					Right precuneus	7	2	73	52	3.93
			1913	0.002	Left superior temporal gyrus	38	22	18	26	3.91
					Left uncus	28	20	5	22	3.51
					Left hippocampus	27	18	33	−1	3.41
	LC	0.040	1165	0.001	Right posterior cingulate	23	6	41	26	3.62
					Left precuneus	7	14	45	31	3.34
					Left posterior cingulate	30	−5	38	18	2.98

Abbreviations: NC, normal controls; AD, Alzheimer's patients; LU, linearization uncorrected images; LC, linearization corrected images; BA, Brodmann's area; K_E, extent voxels

Table 2 Locations and peaks observed in SPM comparing rCBF distribution between LU and LC images

Subject	SPM	Cluster level		Peak voxels				
		K_E	Corrected p	Locations	x	y	z	Z-score
AD	LC > LU	1725	0.000	Right cerebellar cortex	40	60	−31	4.34
		324	0.013	Right basal ganglia	26	8	−2	4.23
		1629	0.000	Left cerebellar cortex	−36	−57	−22	4.20
		392	0.005	Left inferior occipital cortex	−22	−90	1	3.94
	LU > LC	229	0.04	Left uncus	−26	1	−27	4.51
NC	LC > LU	7614	0.000	Right cerebellar cortex	12	−73	−15	6.65
		4709	0.000	Left posterior cingulate cortex	-6	−52	21	5.66
		600	0.000	Right superior temporal cortex	57	−53	16	4.42

Abbreviations: NC, normal controls; AD, Alzheimer's patients; LU, linearization uncorrected images; LC, linearization corrected images; BA, Brodmann's area; K_E, extent voxels

to compare the images. A gray matter threshold 0.7 was selected for the SPM analysis.[10] The CBF data were set for global normalization using proportional scaling to 50. We set the contrast 'NC > AD' to examine the areas of perfusion-deficiency in the AD group to compare the findings with the control group (effect of disease). The same analytical setting was applied for both LU and LC images. Next, a direct SPM comparison between LU and LC images was done in case of both the control and patient groups (2 conditions, 1 scan/condition: paired t-test). The statistical parametric maps of the t statistic, SPM {t}, were then calculated. The SPM {t} values were compared to the threshold using an uncorrected $p < 0.005$ at each voxel. Then, t values were converted into normally distributed Z statistics so that the influence of the degree of freedom (such as the number of images) was normalized. The resulting foci are characterized in terms of spatial extent and peak height. The set of voxels (clusters) with corrected p values below 0.05 were retained as significant. The location of significant differences was evaluated using Talairach's brain atlas, taking into consideration that the shape of Talairach's brain atlas and SPM's template are different.[27]

RESULTS

Pattern of hypoperfusion in mild Alzheimer's disease demonstrated by SPM

In the mild AD patients, SPM with LU images demonstrated significant clusters of hypoperfusion in the left posterior cingulate gyrus, right precuneus, left superior temporal gyrus, left uncus, and left hippocampus (Table 1, Fig. 1) whereas SPM with LC images showed significant clusters of hypoperfusion in the bilateral posterior cingulate gyrus and left precuneus (Fig. 2).

Pattern of rCBF distribution in the ^{99m}Tc-HMPAO SPECT with or without linearization correction

Table 2 summarizes the results of SPM comparing two groups of images in AD and NC subjects, respectively. The contrast, 'LC > LU', showed significantly higher rCBF distribution in the right cerebellum, left inferior occipital cortex, right basal ganglia, and left cerebellum in the LC images of AD patients (Fig. 3a). In the LC images of the control subjects, SPM with the same contrast revealed significantly greater rCBF distribution in the right cerebellum, left posterior cingulate gyrus, right superior temporal gyrus as compared with the corresponding LU images (Fig. 3b). The reverse contrast, 'LU

> LC', showed significantly higher rCBF distribution in the left uncus in the LU images (Fig. 3c) of AD patients. However, such comparison, 'LU > LC' did not reveal any significant change in CBF distribution in the LU images of the control subjects (Fig. 3d).

DISCUSSION

In the present study, SPM demonstrated a significant hypoperfusion at the posterior cingulate and precuneus in mild AD in the cases of both LU and LC images (Fig. 1a and Fig. 1b). However, hippocampal hypoperfusion was detected only on the LU images and could not be observed when LC images were used for the SPM analysis (Table 1).

Hippocampus is one of the brain areas known to be affected the earliest in AD. Braak and Braak[28] defined six stages of AD based on the distribution of neurofibrillary tangles; one of the pathological hallmarks of AD,[29,30] which were reported to be found in the medial temporal cortices and correlated clinically to mild to moderate stages of the disease process.[31–33] Corresponding to the pathological staging, a number of brain perfusion SPECT studies indicated that medial temporal hypoperfusion could be a target of analysis for early detection of AD.[8–14]

Callen[11] reported details of limbic system hypoperfusion occurring in mild AD (MMSE score of 19.5) by means of ^{99m}Tc-HMPAO SPECT without linearization-correction. In a like manner, Nebu[12] also showed bilateral hippocampal hypoperfusion in the early stage of AD (mean MMSE score of 22). On the other hand, Ohnishi[8] correlated the degree of cognitive impairment to the hippocampal hypoperfusion by using ^{99m}Tc-HMPAO SPECT with linearization correction. Although these studies indicated that hippocampal hypoperfusion could be detectable in mild AD, they have used ROI with some a priori hypothesis leaving large areas of brain unexplored. Employing voxel wise analysis with linearization uncorrected images, Johnson[13] demonstrated that decrease in perfusion in the hippocampal-amygdaloid complex was associated with the conversion from questionable (clinical dementia rating 0.5) to probable AD (CDR > 1). In addition, Kemp[10] first applied SPM analysis for ^{99m}Tc-HMPAO SPECT without linearization-correction to differentiate early onset from late onset AD, and detected significantly a greater medial temporal hypoperfusion occurring in late onset AD. A recent SPM study[14] including ^{99m}Tc-ethylene cystine dimer (ECD) SPECT without linearization-correction, reported hypoperfusion in the bilateral parahippocampal and medial temporal cortices, precuneus, posterior cingulate, and parietal association cortices occurring in the mild cognitive-impaired patients (mean MMSE 26.2) who later on, progressed to AD stage (mean MMSE 19.1).[33] On the other hand, using linearization corrected ^{99m}Tc-ECD SPECT, Kogure[9] reported hypoperfusion at the posterior cingulate and precuneus in patients with mild cognitive impairment (mean MMSE score 26.2, CDR 0.5) and that hypoperfusion was additionally detected at the left hippocampus and parahippocampal gyrus in the follow-up patients (mean duration, 15 months) who progressed to the AD stage (mean MMSE score 22.3, CDR 1.0). Although these two studies[9,14] detected hypoperfusion in the parahippocampal gyrus in mild AD by means of SPM with ^{99m}Tc-ECD SPECT, it should be mentioned that the brain distribution patterns of ^{99m}Tc-ECD and ^{99m}Tc-HMPAO in normal control as well as AD patients are differently interpreted by SPM analysis.[34,35] Moreover, Kogure [9] did not include LU images to compare their results with LC images in his study design. Even if LU images were included in Kogure's study, hippocampal hypoperfusion could be reasonably assumed during the stage of mild cognitive impairment in their study population.

Why were LC images unable to reveal medial temporal hypoperfusion in our SPM analysis? Lassen[7] had cautioned already in his early paper that the brain-blood partition coefficient and conversion rate of tracer from brain to blood, which were assumed to be constant in the case of linearization correction algorithm, might not be constant for all parts of the brain and also might vary from patient to patient or in normal to diseased brain regions or presumably, in high flow cortical regions to low-flow cortical regions.[36] Therefore, due to the nonlinear characteristics of the algorithm, the linearization correction method may underestimate rCBF values at the hippocampal cortex, which has a physiologically low blood flow (low flow cortex) in contrast to the posterior cingulate (high flow cortex).[37] Moreover, the absence of any significant hypoperfusion across the hippocampal cortices in SPM with LC is likely due to the brain areas used as the reference, such as the cerebellum for linearization correction and the average whole brain for 'proportional scaling' in SPM. These factors possibly contribute to the rCBF signals in the low flow cortex in the case of the LC images within the SPM work-up and probably neutralize the potential advantage of such an enhanced image contrast method. This speculation was further strengthened when LU and LC images were compared by SPM in our analysis. A greater distribution of rCBF at the high flow cortex was observed in LC images (Fig. 3a, 3b) which indicated that linearization correction improved the nonlinearity (true CBF vs. Count) in the high flow cortices. However, the trend of tracer distribution across the medial temporal cortex was relatively higher in LU images than LC images of the AD patients (SPM significant) (Fig. 3c) and control subjects (SPM non-significant) (Fig. 3d). Although linearization correction yields a more contrasted representation of the distribution of tracer on the ^{99m}Tc-HMPAO SPECT images, to detect the earliest pattern of perfusion abnormalities in mild AD, one should keep in mind that hippocampal hypoperfusion might be

missed when applying LC images for SPM analysis.

In the early stage of AD, hippocampal involvement is long-established, whereas the recent consensus on posterior cingulate connection is increasing, although the mechanisms are yet to be confirmed.[38] In our study, we observed significant hippocampal hypoperfusion in LU images but not in LC images. Therefore, we checked our data by applying different gray matter thresholds (0.6, 0.5, and 0.4) during the analysis with the results found to be consistent at each corresponding threshold. Moreover, posterior cingulate hypoperfusion, which was detected in both LU and LC images, revealed higher z-score in LU images (z = 5.49) than LC images (z = 3.92). Taken together, the present results suggest that the pattern of hypoperfusion in mild AD would be detected by SPM more sensitively in the LU images, in contrast to the LC images.

The limitations of this study should be referred to as well. The size of the study population is limited. However, there is a general agreement that at least ten scans in a group may reveal a reliable result in SPM.[15] Apart from the linearization correction, image reconstruction methods might influence the sensitivity of SPM which should be investigated by future studies.[15] Since this study addressed the effect of linearization correction on SPM, we carefully followed the standard set of image reconstruction parameters implemented by the other relevant studies we discussed.[30,31] For instance, Ohnishi[8] and Nebu[12] applied the attenuation coefficient factors 0.079 cm^{-1} (LC images) and 0.08 cm^{-1} (LU images), respectively. In our study, we applied (LC and LU images) 0.08 cm^{-1} for the image reconstruction, which was referred to as a routine clinical setting after conducting a 20 cm phantom (cylindrical) study in our hospital (unpublished data).

Nevertheless, the present study draws attention to the effect of linearization correction on the detectability of hippocampal hypoperfusion which might be missed when evaluating perfusion abnormalities in mild AD by means of SPM. The pattern of hypoperfusion in mild AD could be detected more sensitively by SPM with LU images than with LC images. The results of SPM may vary in HMPAO SPECT with or without linearization correction, which should be carefully evaluated when interpreting rCBF abnormalities in mild Alzheimer's disease.

ACKNOWLEDGMENTS

The authors acknowledge the expert technical support given by the staff of the two collaborating departments and radioisotope unit. We would also like to thank to Ms. Kayoko Tsunoda and Ms. Maki Sudo for their secretarial help. This study was supported by the grant no. 15390361 from the Ministry of Education, Culture, Sports, Science, and Technology (MEXT), JAPAN.

REFERENCES

1. Dougall NJ, Bruggink S, Ebmeir KP. The clinical use of ^{99m}Tc-HMPAO SPECT in Alzheimer's disease, In: *SPECT in Dementia*. Ebmeir KP (ed), Basel; Karger, 2003: 4–37.
2. Jagust W, Thisted R, Devous MD Sr, Van Heertum R, Mayberg H, Jobst K, et al. SPECT perfusion imaging in the diagnosis of Alzheimer's disease: A clinical pathologic study. *Neurology* 2001; 56: 950–956.
3. Van Gool WA, Walstra GJ, Teunisse S, Van der Zant FM, Weinstein HC, Van Royen EA. Diagnosing Alzheimer's disease in elderly, mildly demented patients: the impact of routine single photon emission computed tomography. *J Neurol* 1995; 242: 401–405.
4. Matsuda H. Cerebral blood flow and metabolic abnormalities in Alzheimer's disease. *Ann Nucl Med* 2001; 15: 85–92.
5. Friston KJ, Holmes AP, Worsely KJ, Poline JP, Frith CD, Frackowiak RSJ. Statistical parametric maps in functional imaging: A general linear approach. *Hum Brain Mapping* 1995; 2: 189–210.
6. Ebmeier KP, Darcourt J, Dougall NJ, Glabus MF. Voxel based approaches in clinical imaging. In: Ebmeir KP (ed). SPECT in Dementia*, Adv Biol Psychiatry*. Basel; Karger, 2003: 72–85.
7. Lassen NA, Andersen AR, Friberg L, Paulson OB. The retention of [^{99m}Tc]-*d*,*l*-HMPAO in human brain after intracarotid bolus injection: A kinetic analysis. *J Cereb Blood Flow Metab* 1988; 8: S13–S22.
8. Ohnishi T, Hoshi H, Nagamachi S, Jinnouchi S, Flores LG II, Futami S, et al. High-resolution SPECT to assess hippocampal perfusion in neuropsychiatric diseases. *J Nucl Med* 1995; 36: 1163–1169.
9. Kogure D, Matsuda H, Ohnishi T, Asada T, Uno M, Kunihiro T, et al. Longitudinal evaluation of early Alzheimer's disease using brain perfusion SPECT. *J Nucl Med* 2000; 41: 1155–1162.
10. Kemp PM, Holmes C, Hoffmann SMA, Bolt L, Holmes R, Rowden J, et al. Alzheimer's disease: differences in technetium-99m HMPAO SPECT scan findings between early onset and late onset dementia. *J Neurol Neurosurg Psychiatry* 2003; 74: 715–719.
11. Callen DJA, Black SE, Caldwell CB. Limbic system perfusion in Alzheimer's disease measured by MRI-coregistered HMPAO SPECT. *Eur J Nucl Med Mol Imaging* 2002; 29: 899–906.
12. Nebu A, Ikeda M, Fukuhara R, Komori K, Maki N, Hokoishi K, et al. Utility of (^{99m})Tc-HMPAO SPECT hippocampal image to diagnose early stages of Alzheimer's disease using semiquantitative analysis. *Dement Geriatr Cogn Disord* 2001; 12: 153–157.
13. Johnson KA MD, Jones K, Holman BL, Becker JA, Spiers PA, Satlin A, et al. Preclinical prediction of Alzheimer's disease using SPECT. *Neurology* 1998; 50: 1563–1571.
14. Hirao K, Ohnishi T, Hirata Y, Yamashita F, Mori T, Moriguchi Y, et al. The prediction of rapid conversion to Alzheimer's disease in mild cognitive impairment using regional cerebral blood flow SPECT. *Neuroimage* 2005; 28: 1014–1021.
15. Lahorte P, Vandenberghe S, Van Laere K, Audenaert K, Lemahieu I, Dierckx RA. Assessing the performance of SPM analyses of SPECT neuroactivation studies.

Neuroimage 2000; 12: 757–764.
16. McKhan G, Drachman D, Folstein M, Katzman R, Price D, Stadlan EM. Clinical diagnosis of Alzheimer's disease: report of the NINCDS-ADRDA Work Group under the auspices of Department of Health and Human Services Task Force on Alzheimer's disease. *Neurology* 1984; 34: 939–944.
17. Hughes CP, Berg L, Danziger WL, Coben LA, Martin RL. A new clinical scale for the staging of dementia. *Br J Psychiatry* 1982; 140: 566–572.
18. Kimura K, Hashikawa K, Etani H, Uehara A, Kozuka T, Moriwaki H, et al. A new apparatus for brain imaging: four-head rotating gamma camera single photon emission computed tomography. *J Nucl Med* 1990; 31: 603–609.
19. Oku N, Matsumoto M, Hashikawa K, Moriwaki H, Ishida M, Seike Y, et al. Intra-individual differences between Technetium-99m-HMPAO and Technetium-99m-ECD in the normal medial temporal lobe. *J Nucl Med* 1997; 38: 1009–1111.
20. Chang LT. A method for attenuation correction in radionuclide computed tomography. *IEEE Trans Nuclear Sci* 1978; NS-25: 638–643.
21. Yoshikawa T, Murase K, Oku N, Kitagawa K, Imaizumi M, Takasawa M, et al. Statistical image analysis of cerebral blood flow in vascular dementia with small-vessel disease. *J Nucl Med* 2003; 44: 505–511.
22. Andersen AR, Friberg HH, Schmidt JF, Hasselbach SG. Quantitative measurements of cerebral blood flow using SPECT and ^{99m}Tc-HMPAO compared to xenon-133. *J Cereb Blood Flow Metab*1988; 8: S69–81.
23. Yonekura Y, Nishizawa S, Mukai T, Fujita T, Fukuyama H, Ishikawa M, et al. SPECT with [^{99m}Tc]-*d*,*l*-Hexamethyl-Propylene Amine Oxime (HMPAO) compared with regional cerebral blood flow measured by PET: Effects of linearization. *J Cereb Blood Flow Metab* 1988; 8: S82–89.
24. Pickut BA, Dierckx RA, Dobbeleir A, Audenaert K, Van Laere K, Vervaet A, et al. Validation of the cerebellum as a reference region for SPECT quantification in patients suffering from dementia of the Alzheimer type. *Psychiatry Res* 1999; 90: 103–112.
25. Sjobeck M, Englund E. Alzheimer's disease and the cerebellum: A morphologic study on neuronal and glial changes. *Dement Geriatr Cogn Disord* 2001; 12: 211–218.
26. Talairach J, Tournoux P. *Co-Planar Stereotactic Atlas of the Human Brain.* Stuttgart: NY; Thieme, 1988.
27. Calder AJ, Lawrence AD, Young AW. Neuropsychology of Fear and Loathing. *Nat Rev Neurosci* 2001; 2: 352–363.
28. Braak H, Braak E. Neuropathological staging of Alzheimer-related changes. *Acta Neuropathol* 1991; 82: 239–259.
29. Selkoe DJ. Cell biology of the amyloid beta-protein precursor and the mechanism of Alzheimer's disease. *Annu Rev Cell Biol* 1994; 10: 373–403.
30. Grundke-Iqbal I, Iqbal K, Tung YC, Quinlan M, Wisniewski HM, Binder LI. Abnormal phosphorylation of the microtubule-associated protein tau (tau) in Alzheimer cytoskeletal pathology. *Proc Natl Acad Sci USA* 1986; 83: 4913–4917.
31. Braak H, Duyckacrts C, Braak E, Piette F. Neuropathological staging of Alzheimer-related changes correlates with psychometrically assessed intellectual status. In: Corain B, Ikbal K, Nicolini M (eds). *Alzheiemer's Disease: Advances in Clinical and Basic Research.* New York; Wiley, 1993: 131–137.
32. Braak H, Braak E, Bohl J. Staging of Alzheimer-related cortical destruction. *Eur Neurol* 1993; 33: 403–408.
33. Gold G, Bouras C, Kovari E, Canuto A, Glaria BG, Malky A, et al. Clinical validity of Braak neuropathological staging in the oldest-old. *Acta Neuropathol* 2000; 99: 579–582.
34. Patterson JC, Early TS, Martin A, Walker MZ, Russell JM, Villanueva-Meyer H. SPECT image analysis using statistical parametric mapping: comparison of technetium-99m-HMPAO and technetium-99m-ECD. *J Nucl Med* 1997; 38: 1721–1725.
35. Koulibaly PM, Nobili F, Migneco O, Vitali P, Robert PH, Girtler N, et al. ^{99m}Tc-HMPAO and ^{99m}Tc-ECD perform differently in typically hypoperfused areas in Alzheimer's disease. *Eur J Nucl Med Mol Imaging* 2003; 30: 1009–1013.
36. Matsuda H, Tsuji S, Shuke N, Sumiya H, Tonami N, Hisada K. Noninvasive measurements of regional cerebral blood flow using technetium-99m hexamethylpropylene amine oxime. *Eur J Nucl Med* 1993; 20: 391–401.
37. Hatazawa J, Fujita H, Kanno I, Satoh T, Iida H, Miura S, et al. Regional cerebral blood flow, blood volume, oxygen extraction fraction, and oxygen utilization rate in normal volunteers measured by the autoradiographic technique and the single breath inhalation method. *Ann Nucl Med* 1995; 9: 15–21.
38. Minoshima S , Giordani B, Berent S, Frey KA, Foster NL, Kuhl DE. Metabolic reduction in the posterior cingulate cortex in very early Alzheimer's disease. *Ann Neurol* 1997; 42: 85–94.